Brain Networks with Modified Connectivity in Patients with Neuropathic Pain and Spinal Cord Injury

Muhammad Abul Hasan[1,2], Aleksandra Vuckovic[3], Parisa Sattar[4], Saad Ahmed Qazi[5,6], Matthew Fraser[7]

[1]Assistant Professor, Department of Biomedical Engineering, NED University of Engineering and Technology, Karachi, Pakistan, Ph. +92(0)21-99230604, Fax: +92(0)21-99261255, Email: abulhasan@neduet.edu.pk.

[2]Co-Principal Investigator, Neurocomputation Laboratory, National Centre for Artificial Intelligence, NED University of Engineering and Technology, Karachi, Pakistan, Ph. +92(0)21-99261261, Fax: +92(0)21-99261255, Email: abulhasan@neduet.edu.pk.

[3]Senior Lecturer, Centre for Rehabilitation Engineering, Biomedical Engineering Division, School of Engineering, University of Glasgow, Glasgow, UK, Ph. +44(0)141 330 3251, Email: Aleksandra.Vuckovic@glasgow.ac.uk

[4]Research Assistant,Neurocomputation Laboratory, National Centre for Artificial Intelligence, NED University of Engineering and Technology, Karachi, Pakistan, Ph. +92(0)21-99261261, Fax: +92(0)21-99261255, Email: parisa@neduet.edu.pk.

[5]Professor, Department of Electrical Engineering, NED University of Engineering and Technology, Karachi, Pakistan, Ph. +92(0)21-99261261, Fax: +92(0)21-99261255, Email: saadqazi@neduet.edu.pk.

[6]Principal Investigator Neurocomputation Laboratory, National Centre for Artificial Intelligence, NED University of Engineering and Technology, Karachi, Pakistan, Ph. +92(0)21-99261261, Fax: +92(0)21-99261255, Email: saadqazi@neduet.edu.pk.

[7]Consultant in Spinal Injury, Queen Elizabeth National Spinal Unit, Southern General Hospital, UK, Ph. +447786264480, Email: Matthew.Fraser@ggc.scott.nhs.uk.

Acknowledgements:

This work was supported by the MRC grant G0902257/1, National Center of Artificial Intelligence. We would like to thank Professor Bernard Conway, University of Strathclyde for lending EEG equipment, and to Dr. Purcell and Dr. Mclean for choosing participants of the study and to all participants for taking part.

Clinical EEG and Neuroscience

Brain Networks with Modified Connectivity in Patients with Neuropathic Pain and Spinal Cord Injury

Journal:	*Clinical EEG & Neuroscience*
Manuscript ID	EEG-20-0132.R1
Manuscript Type:	Review
Keywords:	electroencephalogram (EEG), SpinaI Cord Injury, Functional Connectivity, Neuropathic pain, Motor Imagery, Phased Locked Value

Abstract:

Background: Neuropathic pain (NP) following spinal cord injury (SCI) affect quality of life of almost 40 % of injured population. The modified brain connectivity was reported under different NP conditions. Therefore, brain connectivity was studies in the SCI population with and without NP with the aim to identify networks that are altered due to injury, pain or both.
Methods: The study cohort is classified in three groups, SCI patients with NP, SCI patients without NP, and able-bodied. EEG of each participant was recorded during motor imagery (MI) of paralyzed and painful, and non-paralyzed and non-painful limbs. Phased Locked Value was calculated using Hilbert transform to study altered Functional Connectivity between different regions.
Results: The posterior region connectivity with frontal, fronto-central, and temporal regions is strongly decreased mainly during MI of dominant upper limb (non-paralyzed and non-painful limbs) in SCI no pain group. This modified connectivity is prominent in the alpha and high frequency bands (beta and gamma). Moreover, Oscillatory modified global connectivity is observed in the pain group during MI of painful and paralyzed limb which is more evident between fronto-posterior, frontocentral-posterior, and within posterior and within frontal regions in theta and SMR frequency bands. Cluster coefficient and local efficiency values are reduced in PNP group while increased in PWP group.
Conclusion: The altered theta band connectivity found in the fronto-parietal network along with global increase in local efficiency is a consequence of pain only, while altered connectivity in the beta and gamma bands along with decrease in cluster coefficient values observed in the sensory-motor network are dominantly a consequence of injury only. The outcomes of this study may be used as a potential diagnostic biomarker for the NP. Further, the expected insight holds great clinical relevance in design of neurofeedback-based neurorehabilitation and connectivity-based Brain-Computer Interfaces for SCI patients.

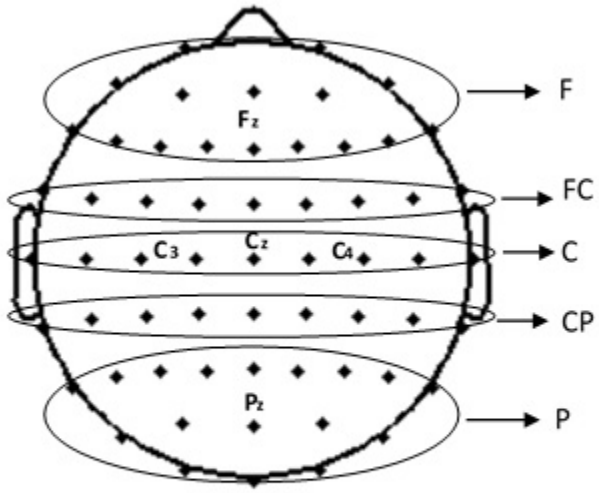

Figure 1

Figure 1: EEG Channels Grouping

128x96mm (96 x 96 DPI)

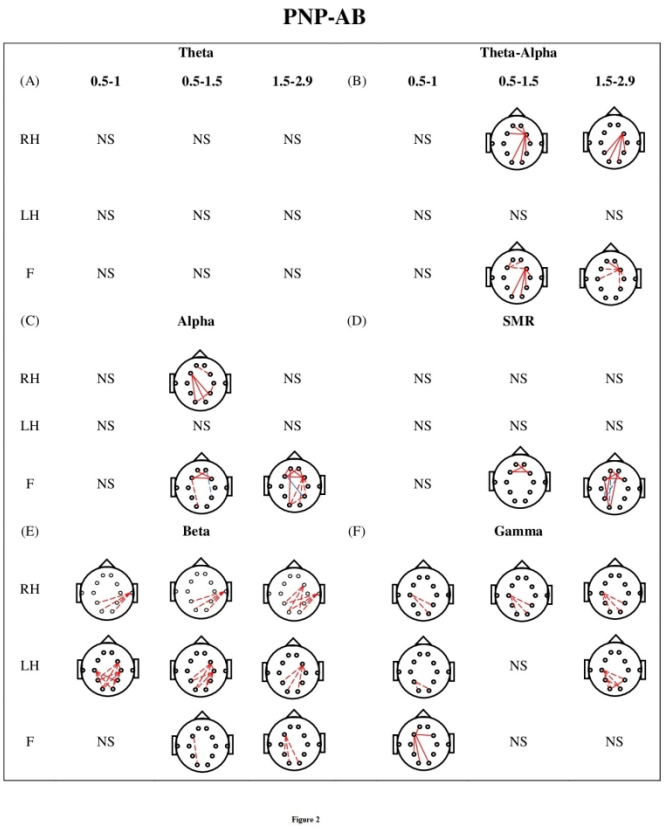

Figure 2

Figure 2: Comparison of Functional Connectivity Strength between Able Bodied (AB) and Patient with No Pain (PNP) during Motor Imagery (MI) of Right Hand (RH), Left Hand (LH) and Foot (F) for different time periods (0.5-1.0 s, 0.5-1.5 s and 1.5-2.9 s) in (A) theta, (B) theta-alpha, (C) alpha, (D) SMR, (E) beta & (F) gamma. Solid lines indicate synchronization in connectivity while dashed lines indicate desynchronization in connectivity. Similarly, red color demonstrates increase de/synchronization in PNP group while blue line demonstrates decrease de/synchronization in PNP group. Moreover, NS represents non significant results.

437x618mm (96 x 96 DPI)

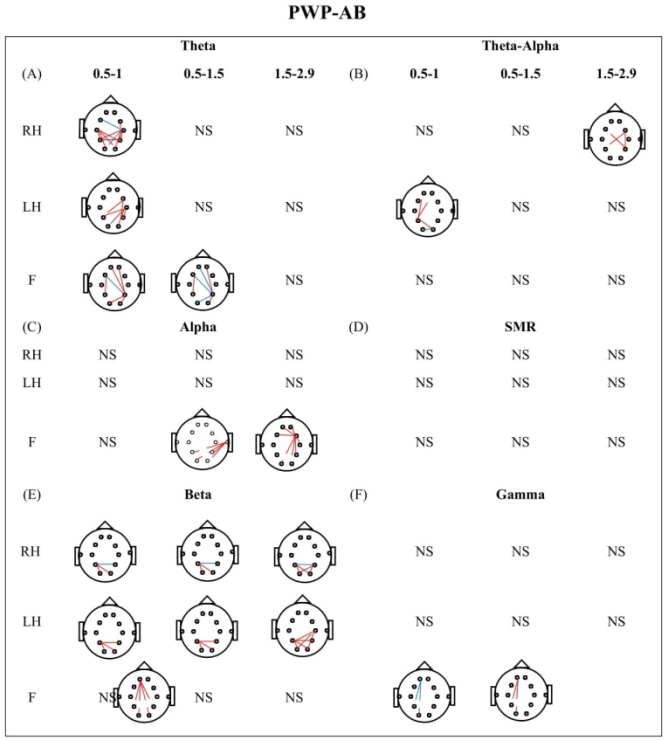

Figure 3

Figure 3: Comparison of Functional Connectivity Strength between Able Bodied(AB) and Patients With Pain (PWP) during Motor Imagery (MI) of Right Hand (RH), Left Hand (LH) and Foot (F) for different time periods (0.5-1.0 s, 0.5-1.5 s and 1.5-2.9 s) in (A) theta, (B) theta-alpha, (C) alpha, (D) SMR, (E) beta & (F) gamma. Solid lines indicate synchronization in connectivity while dashed lines indicate desynchronization in connectivity. Similarly, red color demonstrates increase de/synchronization in PWP group while blue line demonstrates decrease de/synchronization in PWP group. Moreover, NS represents non significant results.

437x618mm (96 x 96 DPI)

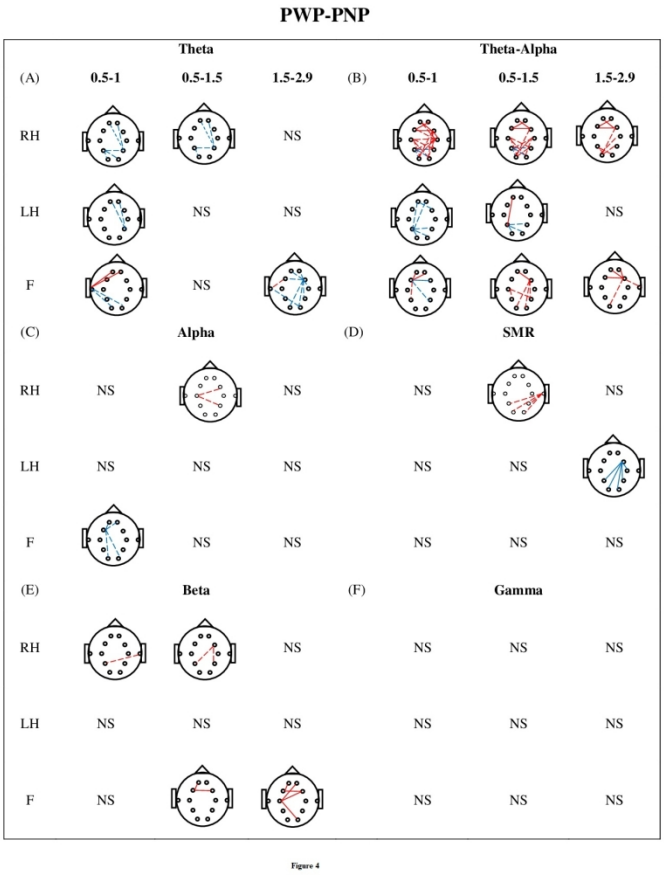

Figure 4

Figure 4: Comparison of Functional Connectivity Strength between Patient with No Pain (PNP) and Patient with Pain (PWP) during Motor Imagery (MI) of Right Hand (RH), Left Hand (LH) and Foot (F) for different time periods (0.5-1.0s, 0.5-1.5s & 1.5-2.9 s) in (A) theta, (B) theta-alpha, (C) alpha, (D) SMR, (E) beta & (F) gamma. Solid lines indicate synchronization in connectivity while dashed lines indicate desynchronization in connectivity. Similarly, red color demonstrates increase de/synchronization in PWP group while blue line demonstrates decrease de/synchronization in PWP group. Moreover, NS represents non significant results.

437x618mm (96 x 96 DPI)

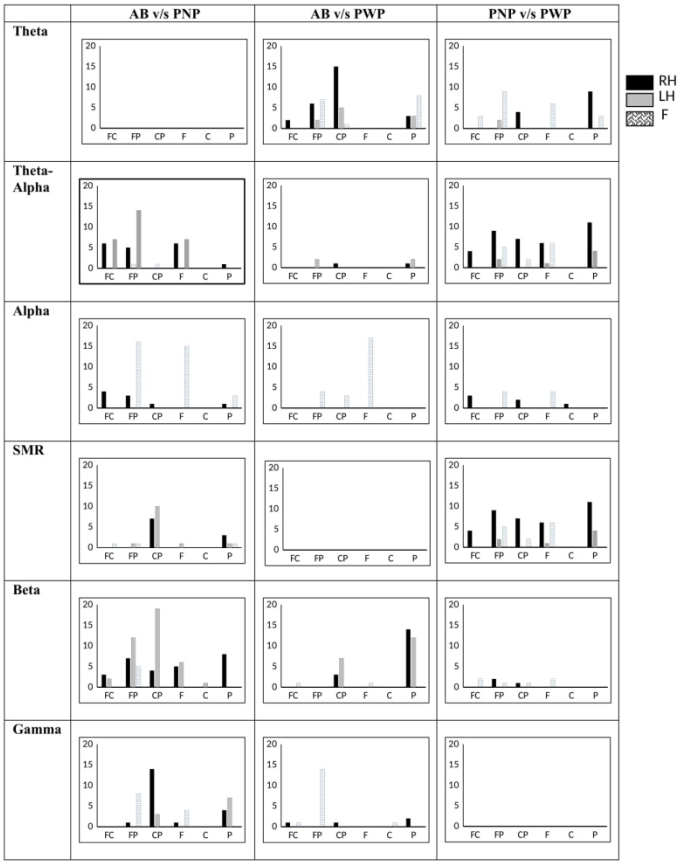

Figure 5: Number of Functional Connections in Able Bodied (AB), Patient with No Pain (PNP) and Patient With Pain (PWP) between Frontal-Central (FC), Frontal-Posterior (FP), Central-Posterior (CP), within Frontal (F), within Central (C) and within Posterior (P) in Theta, Alpha, Beta and Gamma bands.

583x825mm (72 x 72 DPI)

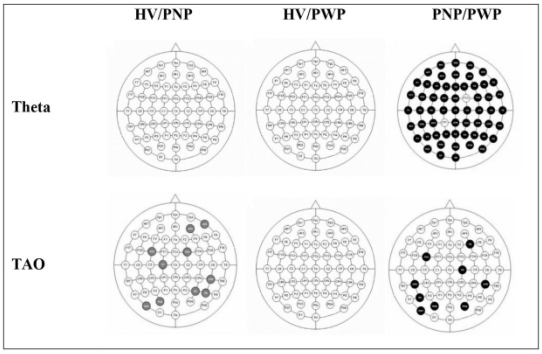

Figure 6

Figure 6: Comparison of Local Efficiency between Able Bodied (AB) & Patient with No Pain (PNP), Able Bodied (AB) & Patient With Pain (PWP) and Patient with No Pain (PNP) & Patient With Pain (PWP) (P = .05) during MI of Foot (F) for time period 0.5-1.0 s in Theta, TAO, Alpha, SMR, Beta & Gamma. Electrode locations marked in black indicate increase in local efficiency whereas, electrode locations marked in grey represent decrease in local efficiency.

210x297mm (300 x 300 DPI)

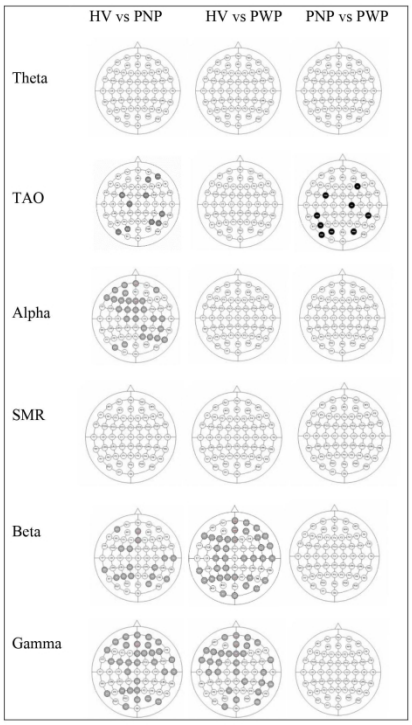

Figure 7

Figure 7: Comparison of Cluster coefficients between Able Bodied (AB) & Patient with No Pain (PNP), Able Bodied (AB) & Patient With Pain (PWP) and Patient with No Pain (PNP) & Patient With Pain (PWP) (P = .05) during MI of Foot (F) for time period 0.5-1.0 s in Theta, TAO, Alpha, SMR, Beta & Gamma. Electrode locations marked in black indicate increase in cluster coefficients whereas, electrode locations marked in grey represent decrease in cluster coefficients.

210x297mm (300 x 300 DPI)

PNP-AB

	Theta			Theta-Alpha			Alpha			SMR			Beta			Gamma		
	RH	LH	F	RH	LH	F	RH	LH	F	RH	LH	F	RH	LH	F	RH	LH	F
Fronto-central				■		■			■			■						
Fronto-posterior									■			■						
Fronto-temporal																		
Frontocentral-posterior				■		■	■		■				■	■	■			■
Temporo-posterior													■					
Within Frontal				■		■	■		■			■						■
Within Central						■												
Within Posterior	■						■										■	
Cental-posterior	■													■		■	■	
Frontocentral-central																		

Table S1: Alteration in Functional Connectivity Strength between PNP v/s AB during MI of RH, LH & F in (A)theta, (B)theta-alpha, (C)alpha, (D)SMR, (E)beta & (F)gamma. Black box indicate alteration in connectivity white box indicate no change in connectivity.

PWP-AB

	Theta			Theta-Alpha			Alpha			SMR			Beta			Gamma		
	RH	LH	F	RH	LH	F	RH	LH	F	RH	LH	F	RH	LH	F	RH	LH	F
Fronto-central																		
Fronto-posterior			■		■													■
Fronto-temporal																		
Frontocentral-posterior	■	■	■	■	■				■									
Temporo-posterior									■									
Within Frontal									■									
Within Central																		
Within Posterior	■		■		■								■	■				
Cental-posterior	■	■												■				
Frontocentral-central																		

Table S2: Alteration in Functional Connectivity Strength between PWP v/s AB during MI of RH, LH & F in (A)theta, (B)theta-alpha, (C)alpha, (D)SMR, (E)beta & (F)gamma. Black box indicate alteration in connectivity white box indicate no change in connectivity.

PWP-PNP

	Theta			Theta-Alpha			Alpha			SMR			Beta			Gamma		
	RH	LH	F	RH	LH	F	RH	LH	F	RH	LH	F	RH	LH	F	RH	LH	F
Fronto-central				■											■			
Fronto-posterior	■	■		■	■													
Fronto-temporal			■			■												
Frontocentral-posterior			■	■		■			■		■		■					
Temporo-posterior			■							■			■					
Within Frontal			■	■	■				■						■			
Within Central				■														
Within Posterior	■			■	■	■												
Cental-posterior				■		■	■								■			
Frontocentral-central			■			■	■				■							

Table S3: Alteration in Functional Connectivity Strength between PWP v/s PNP during MI of RH, LH & F in (A)theta, (B)theta-alpha, (C)alpha, (D)SMR, (E)beta & (F)gamma. Black box indicate alteration in connectivity white box indicate no change in connectivity.

Brain Networks with Modified Connectivity in Patients with Neuropathic Pain and Spinal Cord Injury

Abstract:

Background: Neuropathic pain (NP) following spinal cord injury (SCI) affect quality of life of almost 40 % of injured population. The modified brain connectivity was reported under different NP conditions. Therefore, brain connectivity was studied in the SCI population with and without NP with the aim to identify networks that are altered due to injury, pain or both.

Methods: The study cohort is classified in three groups, SCI patients with NP, SCI patients without NP, and able-bodied. EEG of each participant was recorded during motor imagery (MI) of paralyzed and painful, and non-paralyzed and non-painful limbs. Phased Locked Value was calculated using Hilbert transform to study altered Functional Connectivity between different regions.

Results: The posterior region connectivity with frontal, fronto-central, and temporal regions is strongly decreased mainly during MI of dominant upper limb (non-paralyzed and non-painful limbs) in SCI no pain group. This modified connectivity is prominent in the alpha and high frequency bands (beta and gamma). Moreover, Oscillatory modified global connectivity is observed in the pain group during MI of painful and paralyzed limb which is more evident between fronto-posterior, frontocentral-posterior, and within posterior and within frontal regions in theta and SMR

frequency bands. Cluster coefficient and local efficiency values are reduced in PNP group while increased in PWP group.

Conclusion: The altered theta band connectivity found in the fronto-parietal network along with global increase in local efficiency is a consequence of pain only, while altered connectivity in the beta and gamma bands along with decrease in cluster coefficient values observed in the sensory-motor network are dominantly a consequence of injury only. The outcomes of this study may be used as a potential diagnostic biomarker for the NP. Further, the expected insight holds great clinical relevance in design of neurofeedback-based neurorehabilitation and connectivity-based Brain-Computer Interfaces for SCI patients.

Key words: Spinal Cord Injury, Functional Connectivity, Neuropathic Pain, Motor Imagery and Phased Locked Value

Introduction:

Spinal cord injury (SCI) and neuropathic pain (NP) causes functional changes in various brain regions thereby affects quality of life of almost 40 % of injured population[1–3]. Our previous study reported theta over-activation along with alpha and beta over-activation during motor tasks performed by SCI patients having NP[4]. Studies on other neurological disorders such as Alzheimer, epilepsy, and mild cognitive impairment reported abnormal brain connectivity[5]. Taken together, altered cortical connectivity may also be expected in patients having NP following SCI[6].

NP affects the functional connectivity (FC) in various regions of the brain such as fronto-parietal, sensory-motor, and within motor (among primary, pre, and supplementary motor areas) networks[7–9]. These studies reported increased connectivity strength due to NP[7], which is not restricted to superficial networks but also found in deep cortical structures[9]. This includes increased connectivity of insula and anterior cingulate cortices with prefrontal region[8]. fMRI studies are mostly based on resting state data as it is sensitive to slow oscillations and has poor temporal resolution[6,10–13]. However, cognitive motor processes such as motor imagery (MI) occur at faster time scales. Furthermore, oscillatory activity changes have been reported in peoples having NP[3,14–17]. Therefore, findings of EEG studies are very important. EEG studies on cortical connectivity also provide oscillatory information in specific frequency bands. Moreover, studies also reported increased

connectivity strength in the alpha and beta bands with long-range (between frontal and posterior regions) and short-range connectivity changes (within posterior and within frontal regions)[3,15–17]. Various SCI studies of altered cortical connectivity are based on fMRI data but reported contradicting findings[10–12,18–23]. However, most studies reported decreased connectivity of primary motor and sensory cortices with supplementary motor area (frontal region), visual and somatosensory cortex[10–12,21–23]. EEG studies has also been widely used to investigate altered brain networks of SCI patients in resting and non-resting state, employing motor tasks such as attempting, executing, or imagery of hands and foot. Study reported significant decreased connectivity over the sensorimotor cortex (located over the central and posterior regions) in patients with SCI when compared with healthy subjects. Studies also found that SCI patients had large numbers of cortical connectivity network in which cingulate and supplementary motor areas were identified as an information hub[3,16,17].

Despite of the detailed literature survey we did not find any brain connectivity study conducted on SCI population separating the impact of injury and NP. Therefore, based on findings of connectivity studies conducted only on SCI population and on subjects with NP only, we assume that connectivity changes following SCI may be an effect of NP as well. This study aims to use EEG to identify which modified brain networks connectivity due to SCI and/or due to NP. The expected

insight holds great clinical relevance in design of neurofeedback-based neurorehabilitation and connectivity-based Brain-Computer Interfaces for SCI patients.

Methodology:

Participants: 30 participants aged between (18 and 55 years old) were recruited and divided into three groups:

1. Able-bodied (AB) without history of any neurological disorder (3 Female, 7 Male, age 39.1 ± 10.1{mean ± standard deviation})
2. SCI Patients with No reported Pain (PNP) (2 Female, 8 Male, age 44.4 ± 8.1)
3. SCI Patients With central neuropathic pain (CNP)≥5 on Visual Numerical Scale (VNS). (3 Female, 7 Male, age 45.2 ± 9.1)

The American Spinal Injury Association (ASIA), an Impairment Classification system is used to determine the neurological level of SCI[24]. All patients having pain≥5 were included in the study. Whereas, patients having any chronic (other than CNP) or acute pain such as brain injury or any neurological disorder that can impact the analysis of EEG or may distract the patients to follow the experimental tasks were excluded from the study. All patients have signed informed consent form in addition to ethical permission granted by local health service to perform experimentations.

EEG Recording and Preprocessing: Neuroscan EEG device (Synamp 2, Neuroscan, USA) was used to record the spontaneous and task related EEG data (linked ear reference) with 61 channels placed on head, based on 10-10 system[25]. The sampling frequency was 1000Hz but down sampled to 250 Hz before preprocessing. High-pass filter of 1Hz and band-pass filter of 48-52 Hz were applied before converting EEG data into average reference. However, ICA was applied for extensive removal of noises or non-EEG activities captured during EEG recordings. In this regard Infomax algorithm was chosen for distinguishing brain activity from artefacts such as eye movements, muscle activity and line noise. Further, Infomax algorithm avoid overcorrection which result in good performance for cancelling artefact[26,27]. The bad components or artifact related components were identified on the basis of their morphology, frequency spectrum, topography, and timing[28]. Once the artefact related components are removed, the signal was then reconstructed and then EEG activity of each channel of both datasets (i.e. with and without removal of bad components) were compared on the basis of visual inspection, frequency spectrum, and topography. The component showed maximum activity at the frontopolar region (identified through topography) were removed as it represents eye movement artifact. Similarly, components showed peaks or strong activity around 50 Hz (identified on the basis of spectrum) were also removed for removing line noise. Components that showed very focal activity at frequencies above 20 Hz usually at the lateral electrodes were considered as muscles artefacts and hence removed.

Experiment Study Design: On the day of experiment participants were asked to avoid coffee/alcohol. EEG was recorded in 2 different states: spontaneous and induced activity during cue-based MI. All patients with pain were requested to fill a Brief Pain Questionnaire[29]. Each participant was requested to sit comfortably on the desk while facing computer screen for visual instructions at approximately 1.5m away. Each participant from all groups performed three types of cue-based MI tasks which are imagined movement of right hand (RH), left hand (LH) or foot (F) tapping. They were told to focus at the center point of the screen and execute MI in response to visual cues and avoid any unnecessary movement During each trial a (cross +) cue appeared as a sign of readiness on screen at t=-1s. A sign to initiate the task appeared next to the cross sign displayed as an arrow at t=0s till t=1.25 sec. These arrows have three directions right, left or down denoting MI tasks of RH, LH or F respectively. All participates were instructed to continue the MI task for 3sec (after the initiation sign) till cross sign disappears from the screen. Total 60 trials divided in six sessions were presented randomly for each MI tasks. The length of each trial was 5 sec with 2 sec prior to cue movement and then 3s of cue movement.

Phase Locking Values (PLV): PLV is used to detect phase synchrony in EEG signal for specific frequency band between two recording side. PLV was calculated for all groups and all MI tasks among 61 channel pairs. There are three steps for measuring PLV[30,31]:

Step 1: Select desired frequency band and Filter Order: Following removal of artifacts, EEG data was first filtered using FIR band-pass filter. theta (4-8Hz), theta-alpha overlap (TAO) (6-10 Hz), alpha (8-12 Hz), SMR (16-24 Hz), beta (20-30 Hz) and gamma (35-40 Hz) frequency ranges were selected. Four cycles of desired signals were selected to find the model order. The filter order for different frequency bands was calculated based on Eq 1 and Eq 2[32].

$$\mathrm{T(sec)} = {}^{(\text{no. of cycles})}/_{\mathrm{f\ (Hz)}} \quad \text{Eq (1)}$$

$$\text{Filter order} = \mathrm{F_s} \times \mathrm{t(sec)} \quad \text{Eq (2)}$$

Where, t represents total time in sec, f represents frequency of a particular band in Hz, and F_s is sampling frequency in Hz. Based on Eq (1) and (2), the filter orders for theta, TAO, alpha, SMR, beta and gamma bands were found to be 250, 167, 125, 63, 40 and 25 respectively. The value of f in Eq (1) was set 4 Hz, 6 Hz, 8 Hz, 16 Hz, 25 Hz and 40 Hz for theta, TAO, alpha, SMR, beta and gamma bands respectively.

Step 2: Calculating Instantaneous Phase: Hilbert transform was used for amplitude and frequency calculations and are termed as Instantaneous amplitude, frequency and phase angle[31,33,34].

Step 3: Measuring PLV: PLV is computed among 61 channels (61*61= 3721 pairs) for time length of single epoch i.e. 5 sec (2 sec before and 3 sec after the target stimuli) using Eq (3).

$$PLV_{i,j}(t) = \frac{1}{\mathrm{N}}\left|\sum_{n=1}^{N} \mathrm{e}^{-i(\varphi_{i(t,n)} - \varphi_{j(t,n)})}\right| \quad \text{Eq (3)}$$

Where N= Number of trials, $\varphi_{i(t,n)}$ and $\varphi_{j(t,n)}$ are the instantaneous phases of the i[th] and j[th] electrodes respectively, at each time point (sample) for n trials. $PLV_{i,j}(t)$ is the phase locked value, calculated between electrodes i and j averaged over all trials for all time point (sample).

PLV Normalization: Reference period of -1.5 to -1.1s was adopted as baseline to find whether participants show desynchronization (reduced connectivity strength i.e. negative PLV) or synchronization (increased connectivity strength i.e. positive PLV) during MI tasks (0 to 3s) as compared to baseline. Eq (4) demonstrates normalization of PLV during MI tasks with baseline PLV value. PLV for a baseline period was subtracted with the PLV calculated for three different time ranges (0.5-1s, 0.5-1.5s, and 1.5-2.9s).

$$PLV_{normalized}\% = \frac{(PLV_{MI} - \mu_{baseline})}{\sigma_{baseline}} \quad \text{.....Eq (4)}$$

Where $PLV_{normalized}$ represent either positive (synchronization) or negative (desynchronization) value of PLV in percentage. PLV_{MI} (value of PLV during MI tasks) subtracted from $\mu_{baseline}$ (the average baseline period) and dividing it by $\sigma_{baseline}$ (baseline standard deviation). PLV_{MI} is calculated by taking average of PLV values calculated from Eq (3).

Graph Theory Analysis: In order to further validate the characteristics of brain network obtained through functional connectivity using EEG data, we have calculated various graph theoretical parameters which include clustering coefficient (Cp) and local efficiency (Eloc). These parameters

were calculated by the help of freely available toolbox "Brain Connectivity" (http://www.brain-connectivity-toolbox.net). Nodes were defined as 61 electrodes locations based on 10-10 international system of electrode placement. An association undirected binary matrix was created by selecting connections having normalized PLV value above 30% of the maximum value.

The clustering coefficient " Cp " was determined using Equation 5 and represents the fraction of a node's neighbors which were also neighbors to one another[35].

$$CCp = \frac{1}{n}\sum Cp_i = \frac{1}{n}\sum\left(\frac{2t_i}{k_i(k_i-1)}\right) \quad \text{Eq (5)}$$

where k_i denotes the degree of a node and t_i denotes the number of connections for a given node.

The local efficiency " Eloc" expresses the effectiveness of the node to the elimination of individual nodes and reflected local information transfer among the nodes. Local efficiency was calculated using equation 6[36].

$$Eloc = \frac{1}{n}\sum Eloc_i = \frac{1}{n}\sum\left(\frac{\sum a_{ij}a_{ih}[d_{jh}(N_i)]^{-1}}{k_i-(k_i-1)}\right) \quad \text{Eq (6)}$$

where $Eloc_i$ denotes node's local efficiency, and $d_{jh}(N_i)$ denotes the length of the shortest path between j and h, which only included i's neighbors.

Statistical Analysis:

For comparison of PLV (action-resting), parametric unpaired t-test was applied between groups (PNP vs PWP, AB vs PWP, AB vs PNP). The Shapiro Wilk test was applied before applying parametric statistical analysis to confirm the normal distribution of normalized PLV values, cluster coefficients, and local efficiency. The p-value was set at 0.05. To control for type-I error which may occur due to repetitive measures, false discovery rate was applied on normalized PLV values over all 60 connections for each single electrode. However, for cluster coefficient and local efficiency values, the effect size was calculated to test whether a significant difference between two groups was due to false positive i.e. type-I error. The effect size was calculated between each group for each electrode location. Effect sizes in ranges 0.2-0.49, 0.5-0.79, and larger than 0.8 were considered as small, medium, and large, respectively[37].

Grouping EEG Channels:

To identify the similar traits, PLV results are presented after grouping 61 EEG channels in five different regions. These include central (C), fronto-central (FC), centro-parietal (CP), frontal (F), and posterior (P) regions as represented in Figure-1.

Figure 1: Should be here

Results:

The FC at cortical level during MI of RH, LH and F for different time periods (0.5-1.0s, 0.5-1.5s and 1.5-2.9s) in various frequency bands (theta, TAO, alpha, SMR, beta and gamma bands) are compared between each of two groups (AB vs PNP AB vs PWP, PWP vs PNP) for 61 electrode locations. The results are presented by grouping electrodes for five different regions as shown in Figure-1. Figure-2 illustrates the comparison of FC strength between AB and PNP while performing MI of RH, LH and F for different time periods (0.5-1.0s, 0.5-1.5s and 1.5-2.9s). In TAO band (figure-2B) PNP group demonstrated synchronization while AB group showed desynchronization within frontal at 0.5-1.5s and between frontal-posterior regions at 0.5-1s and 1.5-2.9s during MI of RH. During MI of F, AB group showed desynchronization while PNP group showed synchronization within frontal regions at 0.5-1s and 1.5-2.9s and between frontal-posterior regions at 0.5-1.5s. In alpha band, (figure-2C) during MI of RH, both groups showed desynchronization which is stronger in PNP group between central-posterior regions at 0.5-1.5s. During MI of F, stronger desynchronization and synchronization in PNP group are observed within frontal and between frontal-posterior region (0.5-1.5s and 1.5-2.9s). In SMR (figure-2D), PNP group showed stronger desynchronization within frontal (0.5-1.5s) and between frontal-posterior regions (1.5-2.9s) during MI of F. In beta band (figure-2E), stronger desynchronization in PNP group is observed between temporal-posterior (0.5-2.9s) and between frontocentral-

posterior regions at 1.5-2.9s during MI of RH. During MI of LH, PNP group showed stronger desynchronization between frontocentral-posterior (0.5-2.9s), and between central-posterior regions (0.5-1s and 0.5-1.5s). Moreover, during MI of F, PNP group showed stronger desynchronization between frontocentral-posterior regions (0.5-1.5s and 1.5-2.9s). In gamma band (figure-2F), during MI of RH and LH, stronger desynchronization is observed between central-posterior regions in PNP group except at 0.5-1.5s for MI of LH. Moreover, during MI of F, both groups showed synchronization which is stronger in PNP group between frontal-posterior and within frontal regions at 0.5-1s.

Figure 2: Should be here

Figure-3 depicts strength of FC between AB and PWP during MI of RH, LH and F for 0.5-1.0s, 0.5-1.5s and 1.5-2.9s time periods. In theta band (figure-3A), AB and PWP groups show desynchronization, which is stronger in PWP group within posterior and between central-frontocentral regions during MI of RH at 0.5-1s. During MI of LH, PWP group showed stronger desynchronization between frontocentral-posterior and central-posterior regions at 0.5-1s. Moreover, during MI of F, PWP group showed strong synchronization while AB group showed desynchronization between frontal-posterior regions at 0.5-1s and 0.5-1.5s. In TAO band (figure-3B), PWP group showed stronger desynchronization between frontocentral-posterior at 1.5-2.9s, between frontal-posterior and within posterior region at 0.5-1s during MI of RH and LH

respectively. In alpha band (figure-3C), during MI of F, PWP group showed strong desynchronization compared to AB group within frontal at 1.5-2.9s, between frontal-posterior and temporo-posterior regions at 0.5-1.5s. In beta band (figure-3E), during MI of RH and LH, AB and PWP both groups show desynchronization, which is stronger in PWP group within posterior regions. In gamma band (figure-3F), during MI of F, PWP group showed weaker desynchronization at 0.5-1s followed by stronger desynchronization at 0.5-1.5s and 1.5-2.9s between frontal-posterior regions.

Figure 3: Should be here

Figure 4 illustrates the comparison of FC strength between PNP and PWP while performing MI of LH, RH and F for 0.5-1.0s, 0.5-1.5s and 1.5-2.9s time periods. In theta band (figure-4A), PWP group showed weaker desynchronization within posterior and between frontal-posterior regions during MI of RH at 0.5-1.0s and 0.5-1.5s. During MI of LH, the weaker desynchronization between frontal-posterior region is noticed at t=0.5-1.0s. Moreover, during MI of F, the strength of desynchronization observed in PWP group is weaker than PNP group at 1.5s-2.9s. These differences are found within frontal and between frontal-posterior regions. In TAO band (figure-4B), during MI of RH, PWP group showed stronger desynchronization between frontal-posterior, central-posterior, and within posterior region at 0.5-1.0s, 0.5-1.5s and 1.5-2.9s. During MI of LH, PWP group showed weaker desynchronization between frontal-posterior and within posterior

region at 0.5-1s and 0.5-1.5s. During MI of F, PWP shows stronger desynchronization within frontal and between frontal-parietal region. In alpha band, (figure-4C), during MI of RH, at 0.5-1.5s PWP group showed stronger desynchronization between frontocentral-parietal and central-posterior region. Moreover, during MI of F at 0.5-1s PWP group showed weaker desynchronization between frontal-posterior and within frontal region. In SMR band (figure-4D), during MI of RH at 0.5-1.5s, PWP group showed stronger desynchronization between temporal-posterior region. Moreover, during MI of LH at 1.5-2.9s, both groups showed synchronization which is weaker in PWP group between frontocentral-posterior regions. In beta band (figure-4E), during MI of RH, both groups showed desynchronization between frontocentral-posterior (0.5-1s) and central-posterior region (0.5-1.5s) which is strong in PWP group. Moreover, during MI of F, PWP group showed strong synchronization compare to PNP group within frontal (0.5-1.5s) and between frontal-posterior (1.5s-2.9s) regions.

Figure 4: Should be here

Figure 5 illustrates numbers of significant functional connections observed when comparing PLV between groups (AB vs PNP, AB vs PWP, PWP vs PNP) in theta, TAO, alpha, SMR, beta, and gamma frequency bands during MI of RH, LH and F. In theta band, maximum number of connections are noticed when AB is compared with PWP and PNP is compared to PWP for RH and F MI tasks. While in TAO band, it is observed when AB is compared with PNP and PNP with

PWP groups while performing MI of LH and RH. Likewise, in alpha band, it is observed for all group's combination for F MI tasks. In SMR band significant differences are observed during groups comparison of PNP and PWP while performing MI of RH. However, in beta and gamma bands, significant differences are observed only for AB and PNP groups comparison while performing MI of LH (beta) and RH (gamma). Regarding networks involved in altered connectivity, it is evident that frontal region showed connection with itself and other regions mainly during MI of F while posterior regions showed connections with itself and other regions predominantly during MI of RH and LH .

Figure 5: Should be here

Figure 6 depicts local efficiency between AB and PNP, AB and PWP, and PNP and PWP during MI of F for 0.5-1.0s time period. Gray filled circles represent a significant decrease in local efficiency while black filled circles represent increase in the local efficiency. In the theta band, comparison between PNP and PWP groups shows that PWP exhibits a significant increase in local efficiency in the frontal, fronto-central, central, centro-parietal and posterior regions with a large effect size ($d>0.8$). In TAO band, PNP group showed low value of local efficiency in frontal, central and posterior regions with a large effect size ($d>0.8$) as compared to other two groups. No significant difference in local efficiency was observed between HV and PWP group.

Moreover, in alpha, SMR, beta and gamma bands changes in local efficiency were observed in the occipital region only.

Figure 6: Should be here

Figure 7 shows comparison of cluster coefficient values between each two groups (HV vs PNP, HV vs PWP, and PNP vs PWP) during MI of paralyzed and painful limb i.e. F for a time period 0.5-1.0s in the theta, TAO, alpha, SMR, beta, and gamma bands. Gray filled circles represent a significant decrease in cluster coefficient values while black filled circles represent increase in the cluster coefficient values. A global significant decrease in cluster coefficient value, with an effect size greater than 0.8, in the beta and gamma bands can be noticed in both PNP and PWP groups as compared to HV group. However, this significant reduction in cluster coefficient values is restricted over the sensory-motor cortex in the theta and TAO bands in PNP group as compared to HV. Comparing PWP with HV group, no significant difference could be noticed. Comparing PWP with PNP group, significant increase in cluster coefficient values could be observed, mainly over the sensory-motor cortex, in the TAO band only, having an effect size greater than 0.8;.

Figure7: Should be here

Discussion:

The objective of this study is to find altered brain networks connectivity due to SCI only and due to NP following SCI. Prominent changes are observed within the sensory motor network i.e. (between central-posterior and between frontocentral-posterior regions) during MI of upper dominant and non-painful limb and in the fronto-parietal network during MI of paralyzed and painful limb. We found that connectivity changes in the theta and SMR bands are mainly due to pain. However, the connectivity changes due to injury are mainly found in the alpha, beta, and gamma bands during MI of painful and non-painful limbs. Furthermore, global increase in local efficiency in the theta band is mainly an effect of pain while localized, restricted to sensory-motor cortex, decrease in local efficiency in the TAO band is mainly an effect of an injury.

A study conducted on SCI people found that alteration in connectivity strength and distinction in functionally connected regions are changed with time since injury[13]. Moreover, studies conducted on pain patients reported association of modified connectivity with pain intensity and perception[8,10,12]. Since, in our study, there are two distinct groups separating injury and pain. Therefore, strongest connectivity decrease in pain group as compared to other two groups suggest that altered connectivity might not only be related to onset of injury but also due to development of pain. Past studies on SCI subjects do not separate the effect of NP when studying brain connectivity and are mainly based on fMRI[10–12,18–23]. EEG studies as compared to fMRI studies

provide frequency specific changes[3,16,17]. Hence, this is the first study showing that connectivity changes in the theta and SMR bands may be biomarker of NP in peoples with SCI. Whilst altered connectivity in the alpha, beta, and gamma bands may be considered as a consequence of SCI only.

The strong connectivity strength decrease within the sensory-motor network of the ascending nociceptive pathway in both SCI groups is in line with findings reported in fMRI studies[14,38,39]. This may be associated with posterior shift of sensory-motor cortex or invasion of cortical representation of affected limb (i.e. paralyzed limb) by unaffected limb (i.e. upper limbs). However, it is required to perform study on tetraplegic patients to confirm. The decrease in connectivity within the sensory-motor networks demonstrates loss in communication between sensory and motor cortices[6,7]. This means SCI participants need lot of attention to understand sensory stimulus and to perform tasks. This is further supported by decrease in cluster coefficient values in the PNP group as compared to other two groups. Altered sensorimotor connectivity is also a direct consequence of lifestyle changes in motor behavior following pain. Therefore, the decreased sensorimotor connectivity may be primarily attributed due to top down control of descending pain pathways.

The salience network (SN) have role in both task execution and pain processing[40–42]. The role of SN in terms of task is to activate the executive network and deactivate the DMN network during

visual or auditory stimulus[43]. The SN is strongly activated in rest to task switch state as compared to task to task switch state[44]. SN is categorized as frontal region for this study[43,45–47]. A study reported strong association of chronic pain (CP) with alteration in SN[40]. Similarly, study reported significant increased SN connectivity due to higher pain intensity[48]. The increased connectivity observed within frontal and fronto-central region demonstrates that PWP group seek strong attention during execution of paralyzed and painful limbs as compared to MI of non-paralyzed and non-painful limbs. Hence, this altered connectivity in SN demonstrates modulation of interoceptive brain processes such as homeostatic regulation of body physiology controlled by integration of internal and external stimuli.

Compound limb MI causes higher activation and coupling of multiple brain networks[49]. The large numbers of connections together with increased value of cluster coefficient in PWP group, in this study, reveals complexity of cognitive process and thereby demonstrates that execution of paralyzed and painful limb is a complex task for PWP group[49]. The fronto-parietal network is considered a functional hub which shows connections with several brain regions[50–52] comprising of frontal (Fp1, Fp2;BA10, F3, F4;BA9, FZ;BA8), temporal (F7, BA47) and parietal regions (P3, P4, BA39)[53]. Frontal cortex plays an important role for performing and controlling cognitive functions by integrating complex perceptual information from sensory-motor cortices. The interaction within posterior region is useful for performing higher cognitive functions such as

updating postural representations of limbs[54]. It is interesting to note that connectivity differences are long-range distance (between frontal-posterior regions) during MI of F. The augmented connectivity within and between fronto-parietal network has been reported in pain and diseases (depression, schizophrenia, anxiety) compromising cognitive functions[55–60]. The altered connectivity within frontal and between frontal-parietal regions has also been reported in patients with different types of CP[7,14,15,61–63]. Therefore, the augmented connectivity, during MI of F limb in both injury and pain groups, reported in this study is either due to injury, pain perception or impaired cognitive functions. Further, the connectivity changes between frontal-posterior regions may reflect an involvement of multiple regions for information exchange.

The default mode network (DMN) comprises of medial prefrontal cortex and medial posterior cortex[64] (i.e. FP1, FP2, FPz, F3, F4, F7, Fz, T3, T4, P3, P4)[53]. The DMN which is part of dynamic pain connectome and large-brain network is active in resting state while inactive during task state. However, few studies reported activation of DMN in task execution when cognitive load increases[65–67]. Studies also reported decreased connectivity in DMN during task performance[65–70]. The connectivity is strongly attenuated in attention demanding task-task initiation[71] because DMN is coupled with fronto-parietal network during task initiation[70,72–74]. The connectivity changes in DMN found in this study during MI of F demonstrate that PWP group faced difficultly in task performance but are highly engaged in attention demanding task. In other words, the

patients focus may be shifted during on-going task towards pain or injury[75]. Therefore, the increase local efficiency in pain group may reflect increased activity in pain matrix neural processing.

Study also reported that the long-range connectivity between frontal-parietal regions is observed when visual and sensory motor brain areas are involved in executing motor tasks that require visual stimulus which is strong in theta band[76]. This varied connectivity may reflect sustained attention to bodily sensations and hypervigilance to somatic sensations. Pain processing region establishes the relationship between pain and decision making relevant to pain. Therefore, additional burden of decision making and processing of desired action responses with CP distractors is reflected with increased connectivity between frontal-posterior regions[21]. The augmented FC in the posterior region (part of pain matrix) reported in this study is likely to reflect expansion due to hyper-perfusion of the signals as reported in fibromyalgia patients[77]. CP causes a paradigm shift towards augmented activation in the brain related to cognitive affecting processing.

Large numbers of nodes are observed in our study during MI of F which demonstrate the involvement of larger neural network in information processing. Multiple nodes are formed at frontal and posterior regions when comparing SCI patients with AB, while at frontal side only when comparing both injury groups. However, previous studies reported formation of large

numbers of nodes only at frontal region in SCI patients as compared to AB[16,21]. In an attempt to move paralyzed and painful limb, more cortical resources are utilized in order to restore the sensation and structural alignment of limb[18,78]. It means that SCI patients showed functional independence of motor cortices for paralyzed limb movement. Formation of nodes at posterior side suggests an enhancement in visual-related sensory processing after loss of spinal afferents[50–52]. This concludes that formation of nodes at posterior region might be due to injury while formation of node at frontal region might be due to pain.

Studies reported theta band overactivation of the pain matrix associated with thalamocortical dysrhythmia (TCD)[79–85]. Moreover, studies reported that the abnormal theta oscillation is the point of interest in various neuropsychiatric disorders such as, in NP thalamic theta oscillation deafferentation entrain thalamocortical loop[82–85]. Thalamocortical loop plays a vital role in encrypting information of sensory-discriminative properties of painful stimuli. Hence, in this study, altered theta band connectivity, ~~and~~ formation of large numbers of nodes, and large local efficiency in theta band reported in pain group as compared to other two groups strongly support the concept of TCD ~~and further demonstrate the decreased information flow between the cortical and thalamic somatosensory areas~~ [82–85].

This study has some limitations. First, we only considered the comparison of pain presence or absence, irrespective of pain intensity which can significantly affect FC. Second, study recruit

only paraplegic patients with CNP, therefore, the findings cannot be generalized for all SCI patients having pain. Third, we analyzed FC of SCI patients without considering duration of injury and pain which can be potential parameters to impact FC.

In conclusion, this study found altered connectivity in fronto-parietal with global increase in local efficiency and modified sensory-motor networks evident with decrease in cluster coefficient values during MI of F (painful and paralyzed limb) which can be used as a potential biomarker for the diagnosis of pain following SCI. Altered brain connectivity in theta bands is associated with pain only, whereas, gamma and beta frequency bands are associated with injury only. It is also observed that numbers of nodes in PWP group are more in theta band during MI of paralyzed and painful limbs. The findings of our study can be used for designing and setting connectivity-based protocols of neuromodulation devices largely used in the field of BCI, neuro-stimulation, neurorehabilitation, neuro-feedback software design, and assistive technologies for SCI and pain patients.

References:

1. Lee S, Zhao X, Hatch M, Chun S, Chang E. Central neuropathic pain in spinal cord injury. *Crit Rev Phys Rehabil Med*. 2013;25(3-4):159-172.
2. Hagen EM, Rekand T. Management of neuropathic pain associated with spinal cord injury. *Pain Ther*. 2015;4(1):51-65.
3. Athanasiou A, Terzopoulos N, Pandria N, et al. Functional brain connectivity during multiple motor imagery tasks in spinal cord injury. *Neural Plast*. 2018;2018:16-21.
4. Vuckovic A, Hasan MA, Fraser M, Conway BA, Nasseroleslami B, Allan DB. Dynamic oscillatory signatures of central neuropathic pain in spinal cord injury. *J Pain*. 2014;15(6):645-655.
5. Freund P, Curt A, Friston K, Thompson A. Tracking changes following spinal cord injury: Insights from neuroimaging. *Neuroscientist*. 2013;19(2):116-128.
6. Freund P, Weiskopf N, Ashburner J, et al. MRI investigation of the sensorimotor cortex and the corticospinal tract after acute spinal cord injury: A prospective longitudinal study. *Lancet Neurol*. 2013;12(9):873-881.
7. Flodin P, Martinsen S, Altawil R, et al. Intrinsic brain connectivity in chronic pain: A resting-state fMRI study in patients with rheumatoid arthritis. *Front Hum Neurosci*. 2016;10(MAR2016).
8. Lee MJ, Park BY, Cho S, Kim ST, Park H, Chung CS. Increased connectivity of pain matrix in chronic migraine: A resting-state functional MRI study. *J Headache Pain*. 2019;20(1).
9. Mutso AA, Petre B, Huang L, et al. Reorganization of hippocampal functional connectivity with transition to chronic back pain. *J Neurophysiol*. 2014;111(5):1065-1076.
10. Hawasli AH, Rutlin J, Roland JL, et al. Spinal cord injury disrupts resting-state

networks in the human brain. *J Neurotrauma*. 2018;35(6):864-873.

11. Oni-Orisan A, Kaushal M, Li W, et al. Alterations in cortical sensorimotor connectivity following complete cervical spinal cord injury: A prospective resting-state fMRI study. *PLoS One*. 2016;11(3):1-13.
12. Hou J, Xiang Z, Yan R, et al. Motor recovery at 6 months after admission is related to structural and functional reorganization of the spine and brain in patients with spinal cord injury. *Hum Brain Mapp*. 2016;37(6):2195-2209.
13. Min Y-S, Chang Y, Park JW, et al. Change of brain functional connectivity in patients with spinal cord injury: graph theory based approach. *Ann Rehabil Med*. 2015;39(3):374-383.
14. Nickel MM, Ta Dinh S, May ES, et al. Neural oscillations and connectivity characterizing the state of tonic experimental pain in humans. *Hum Brain Mapp*. 2019;(May):1-13.
15. Ye Q, Yan D, Yao M, Lou W, Peng W. Hyperexcitability of cortical oscillations in patients with somatoform pain disorder: resting-state EEG study. *Neural Plast*. 2019;2019:2687150.
16. De Vico Fallani F, Astolfi L, Cincotti F, et al. Cortical functional connectivity networks in normal and spinal cord injured patients: Evaluation by graph analysis. *Hum Brain Mapp*. 2007;28(12):1334-1346.
17. De Vico Fallani F, Astolfi L, Cincotti F, et al. Brain connectivity structure in spinal cord injured: Evaluation by graph analysis. *Annu Int Conf IEEE Eng Med Biol - Proc*. Published online 2006:988-991.
18. Cramer SC, Lastra L, Lacourse MG, Cohen MJ. Brain motor system function after chronic, complete spinal cord injury. *Brain*. 2005;128(12):2941-2950.

19. Kaushal M, Oni-orisan A, Chen G, et al. Large-scale network analysis of whole-brain resting-state functional connectivity in spinal cord injury: A comparative study. *Brain Connect*. 2017;7(7):413-423.
20. Wrigley PJ, Gustin SM, Macey PM, et al. Anatomical changes in human motor cortex and motor pathways following complete thoracic spinal cord injury. *Cereb Cortex*. 2009;19(1):224-232.
21. Hou QJ, Sun T, Xiang Z, Zhang J, Zhang Z. Alterations of resting-state regional and network-level neural function after acute spinal cord injury. *Neuroscience*. 2014;277:446-454.
22. Rao JS, Liu Z, Zhao C, et al. Longitudinal evaluation of functional connectivity variation in the monkey sensorimotor network induced by spinal cord injury. *Acta Physiol*. 2016;217(2):164-173.
23. Kaushal M, Oni-orisan A, Chen G, et al. Evaluation of whole-brain resting-state functional connectivity in spinal cord injury – a large-scale network analysis using network-based statistic. *J Neurotrauma*. 2016;34(6):1-16.
24. Burns S, Biering-Sørensen F, Donovan W, et al. International standards for neurological classification of spinal cord injury, revised 2011. *Top Spinal Cord Inj Rehabil*. 2012;18(1):85-99.
25. Lesser R, Picton TW. American Electroencephalographic Society Guidelines for Standard Electrode Position Nomenclature. *J Clin Neurophysiol*. 1991;8(2):200-202.
26. Frølich L, Dowding I. Removal of muscular artifacts in EEG signals: a comparison of linear decomposition methods. *Brain Informatics*. 2018;5(1):13-22.
27. Dimigen O. Optimizing the ICA-based removal of ocular EEG artifacts from free viewing experiments. *Neuroimage*. 2020;207(January 2019):116117.

28. Chaumon M, Bishop DVM, Busch NA. A practical guide to the selection of independent components of the electroencephalogram for artifact correction. *J Neurosci Methods*. 2015;250:47-63.
29. Daut RL, Cleeland CS, Flanery RC. Development of the Wisconsin Brief Pain Questionnaire to assess pain in cancer and other diseases. *Pain*. 1983;17(2):197-210.
30. Lachaux J, Rodriguez E, Martinerie J, Varela FJ. Measuring phase synchrony in brain signals. 1999;208:1-15.
31. Jian W, Chen M, McFarland DJ. EEG based zero-phase phase-locking value (PLV) and effects of spatial filtering during actual movement. *Brain Res Bull*. 2017;130:156-164.
32. Hamner B, Leeb R, Tavella M, Del R. Millán J. Phase-based features for motor imagery brain-computer interfaces. In: *2011 Annual International Conference of the IEEE Engineering in Medicine and Biology Society*. IEEE; 2011:2578-2581.
33. Bakhshayesh H, Fitzgibbon SP, Janani AS, Grummett TS, Pope KJ. Detecting synchrony in EEG: A comparative study of functional connectivity measures. *Comput Biol Med*. 2019;105:1-15.
34. Bruns A. Fourier- , Hilbert- and wavelet-based signal analysis : are they really different approaches ? *J Neurosci Methods*. 2004;137:321-332.
35. Strogatz DJW& SH. Collective dynamics of 'small-world' networks Duncan. *Conserv Biol*. 2018;32(2):287-293.
36. Latora V, Marchiori M. Efficient behavior of small-world networks. *Phys Rev Lett*. 2001;87(19):198701-1-198701-198704.
37. Hedges L V. Distribution Theory for Glass ' s Estimator of Effect Size and Related Estimators Author (s): Larry V . Hedges Published by : American Educational

Research Association and American Statistical Association Journaet o Educational Statis6tiL Key Words : Me. 2014;6(2):107-128.

38. Gustin SM, Peck CC, Cheney LB, Macey PM, Murray GM, Henderson LA. Pain and plasticity: Is chronic pain always associated with somatosensory cortex activity and reorganization? *J Neurosci*. 2012;32(43):14874-14884.
39. Henderson LA, Gustin SM, Macey PM, Wrigley PJ, Siddall PJ. Functional reorganization of the brain in humans following spinal cord injury: Evidence for underlying changes in cortical anatomy. *J Neurosci*. 2011;31(7):2630-2637.
40. Hemington KS, Wu Q, Kucyi A, Inman RD, Davis KD. Abnormal cross-network functional connectivity in chronic pain and its association with clinical symptoms. *Brain Struct Funct*. 2016;221(8):4203-4219.
41. Seeley WW, Menon V, Schatzberg AF, et al. Dissociable intrinsic connectivity networks for salience processing and executive control. *J Neurosci*. 2007;27(9):2349-2356.
42. Di X, Biswal BB. Dynamic brain functional connectivity modulated by resting-state networks. *Brain Struct Funct*. 2015;220(1):37-46.
43. Sridharan D, Levitin DJ, Menon V. A critical role for the right fronto-insular cortex in switching between central-executive and default-mode networks. *Pnas*. 2008;105(34):12569-12574.
44. Sidlauskaite J, Wiersema JR, Roeyers H, et al. Anticipatory processes in brain state switching — Evidence from a novel cued-switching task implicating default mode and salience networks. *Neuroimage*. Published online 2014.
45. Marek S, Dosenbach NUF. Control networks of the frontal lobes. *Front Lobes*. 2019;163:333-347.

46. Gogolla N. The insular cortex. *Curr Biol*. 2017;27(12):R580-R586.
47. Heilbronner SR, Hayden BY. Dorsal Anterior Cingulate Cortex : A Bottom-Up View. *Annu Rev ofNeuroscience*. 2016;39:149-170.
48. Ettinger- H Van, Södermark M, Graven-nielsen T, Sjörs A, Engström M, Gerdle B. Chronic widespread pain patients show disrupted cortical connectivity in default mode and salience networks , modulated by pain sensitivity. *J ofPain Res*. 2019;12:1743-1755.
49. Yi W, Qiu S, Wang K, et al. Evaluation of EEG oscillatory patterns and cognitive process during simple and compound limb motor imagery. *PLoS One*. 2014;9(12):1-19.
50. Cole MW, Pathak S, Schneider W. Identifying the brain's most globally connected regions. *Neuroimage*. 2010;49(4):3132-3148.
51. Power JD., Schlaggar BL., Lessov-Schlaggar CN. PS. Evidence for hubs in human functional brain networks. *Neuron*. 2013;79(4):798–813.
52. Marek S, Hwang K, Foran W, Hallquist MN, Luna B. The Contribution of Network Organization and Integration to the Development of Cognitive Control. *PLoS Biol*. 2015;13(12):1-25.
53. Rojas GM, Alvarez C, Montoya CE, Iglesia-vayá M De, Cisternas JE, Gálvez M. Study of resting-state functional connectivity networks using EEG electrodes position as seed. 2018;12:235.
54. Hétu S, Grégoire M, Saimpont A, et al. Neuroscience and Biobehavioral Reviews The neural network of motor imagery : An ALE meta-analysis. *Neurosci Biobehav Rev*. 2013;37(5):930-949.
55. Sylvester CM., Barch DM., Corbetta M., Power JD., Schlaggar BL. LJ. Resting State

Functional Connectivity of the Ventral Attention Network in Children With a History of Depression or Anxiety. *J Am Acad Child Adolesc Psychiatry*. 2013;52(12):326–1336.

56. Heinrichs RW, Zakzanis KK. Neurocognitive deficit in schizophrenia: A quantitative review of the evidence. *Neuropsychology*. 1998;12(3):426-445.
57. Sheffield JM, Kandala S, Tamminga CA, et al. Transdiagnostic associations between functional brain network integrity and cognition. *JAMA Psychiatry*. 2017;74(6):605-613.
58. Dominici et al. Variable Global Dysconnectivity and Individual Differences in Schizophrenia. *Biol Psychiatry*. 2011;70(1):43–50.
59. Anticevic A, Repovs G, Barch DM. Working memory encoding and maintenance deficits in schizophrenia: Neural evidence for activation and deactivation abnormalities. *Schizophr Bull*. 2013;39(1):168-178.
60. Repovs G., Csernansky JG. BD. Brain Network Connectivity in Individuals with Schizophrenia and their Siblings. *Biol Psychiatry*. 2011;69(10):967–973.
61. Baliki MN, Petre B, Torbey S, et al. Corticostriatal functional connectivity predicts transition to chronic back pain. *Nat Neurosci*. 2012;15(8):1117-1119.
62. Seminowicz DA, Mikulis DJ, Davis KD. Cognitive modulation of pain-related brain responses depends on behavioral strategy. *Pain*. 2004;112(1-2):48-58.
63. Moore DJ, Eccleston C, Keogh E. Cognitive load selectively influences the interruptive effect of pain on attention. *Pain*. 2017;158(10):2035-2041.
64. Raichle ME, Macleod AM, Snyder AZ, Powers WJ, Gusnard DA, Shulman GL. A default mode of brain function. *Pnas*. 2001;98(2):676-682.
65. Newton AT, Morgan VL, Rogers BP, Gore JC. Modulation of Steady State Functional

Connectivity in the Default Mode and Working Memory Networks By Cognitive Load. *Hum Brain Mapp 321649–1659*. 2011;32:1649-1659.

66. Mohammad R. Arbabshirani, Martin Havlicek, Kent A. Kiehl GDP and VDC. Functional network connectivity during rest and task conditions: A comparative study Mohammad. *Hum Brain Mapp*. 2013;34(11):1-24.
67. Vatansever D, Menon DK, Manktelow AE, Sahakian BJ, Stamatakis EA. Default mode network connectivity during task execution. *Neuroimage*. 2015;122:96-104.
68. Herna R, Deus J, Ortiz H, et al. Consistency and functional specialization in the default mode brain network. *Pnas*. 2008;105(28):9781-9786.
69. Fransson P, Marrelec G. The precuneus / posterior cingulate cortex plays a pivotal role in the default mode network : Evidence from a partial correlation network analysis. *Neuroimage*. 2008;42:1178-1184.
70. Spreng RN, Sepulcre J, Turner GR, Stevens WD, Schacter DL. Intrinsic Architecture Underlying the Relations among the Default , Dorsal Attention , and Frontoparietal Control Networks of the Human Brain. *J Cogn Neurosci*. 2012;25(1):74-86.
71. Fransson P. How default is the default mode of brain function ? Further evidence from intrinsic BOLD signal fluctuations. *Neuropsychologia*. 2006;44:2836-2845.
72. Spreng RN, Stevens WD, Chamberlain JP, Gilmore AW, Schacter DL. Default network activity , coupled with the frontoparietal control network , supports goal-directed cognition. *Neuroimage*. 2010;53(1):303-317.
73. Leech R, Kamourieh S, Beckmann CF, Sharp DJ. Fractionating the default mode network : distinct contributions of the ventral and dorsal posterior cingulate cortex to cognitive control. *J Neurosci*. 2011;31(9):3217-3224.
74. Margulies DS, Vincent JL, Kelly C, et al. Precuneus shares intrinsic functional

architecture in humans and monkeys. *Pnas*. 2009;106(47):20069–20074.

75. Gustin SM, Wrigley PJ, Siddall PJ, Henderson LA. Brain anatomy changes associated with persistent neuropathic pain following spinal cord injury. *Cereb Cortex*. 2010;20:1409-1419.
76. Cooper PS, Wong ASW, Fulham WR, et al. Theta frontoparietal connectivity associated with proactive and reactive cognitive control processes. *Neuroimage*. 2015;108:354-363.
77. Fallon N, Chiu Y, Nurmikko T, Stancak A. Functional connectivity with the default mode network is altered in fibromyalgia patients. *PLoS One*. 2016;11(7):1-12.
78. De Vico Fallani F, Astolfi L, Cincotti F, et al. Extracting information from cortical connectivity patterns estimated from high resolution EEG recordings: A theoretical graph approach. *Brain Topogr*. 2007;19(3):125-136.
79. Alshelh Z, di Pietro F, Youssef AM, et al. Chronic neuropathic pain: It's about the rhythm. *J Neurosci*. 2016;36(3):1008-1018.
80. Sarnthein J, Stern J, Aufenberg C, Rousson V, Jeanmonod D. Increased EEG power and slowed dominant frequency in patients with neurogenic pain. *Brain*. 2006;129(1):55-64.
81. Stern J, Jeanmonod D, Sarnthein J. Persistent EEG overactivation in the cortical pain matrix of neurogenic pain patients. *Neuroimage*. 2006;31(2):721-731.
82. Llinás RR, Ribary U, Jeanmonod D, Kronberg E, Mitra PP. Thalamocortical dysrhythmia: A neurological and neuropsychiatric syndrome characterized by magnetoencephalography. *Proc Natl Acad Sci U S A*. 1999;96(26):15222-15227.
83. Llinás R, Urbano FJ, Leznik E, Ramírez RR, Van Marle HJF. Rhythmic and dysrhythmic thalamocortical dynamics: GABA systems and the edge effect. *Trends*

Neurosci. 2005;28(6):325-333.

84. Llinás R, Ribary U, Jeanmonod D, et al. Thalamocortical dysrhythmia I . Functional and imaging aspects. *Thalamus Relat Syst*. 2001;1:237-244.

85. Jeanmonod D, Magnin M, Morel A, et al. Thalamocortical dysrhythmia II. Clinical and surgical aspects. *Thalamus Relat Syst*. 2001;1:245-254.

List of Figures:

Central-Posterior (CP), within Frontal (F), within Central (C) and within Posterior (P) in Theta, Alpha, Beta and Gamma bands.

Figure 6: Comparison of Local Efficiency between Able Bodied (AB) & Patient with No Pain (PNP), Able Bodied (AB) & Patient With Pain (PWP) and Patient with No Pain (PNP) & Patient With Pain (PWP) (P = .05) during MI of Foot (F) for time period 0.5-1.0 s in Theta, TAO, Alpha, SMR, Beta & Gamma. Electrode locations marked in black indicate increase in local efficiency whereas, electrode locations marked in grey represent decrease in local efficiency.

Figure 7: Comparison of Cluster coefficients between Able Bodied (AB) & Patient with No Pain (PNP), Able Bodied (AB) & Patient With Pain (PWP) and Patient with No Pain (PNP) & Patient With Pain (PWP) (P = .05) during MI of Foot (F) for time period 0.5-1.0 s in Theta, TAO, Alpha, SMR, Beta & Gamma. Electrode locations marked in black indicate increase in cluster coefficients whereas, electrode locations marked in grey represent decrease in cluster coefficients.